AGU PUBLICATIONS

JGR

Journal of Geophysical Research: Atmospheres

RESEARCH ARTICLE
10.1002/2014JD021454

Key Points:
- Vegetation changes impacted precipitation more than soil moisture changes
- Soil moisture changes had a larger impact on temperature and humidity
- Opposite impacts on temperature and humidity created minimal convective changes

Correspondence to:
T. W. Collow,
tcollow@envsci.rutgers.edu

Citation:
Collow, T. W., A. Robock, and W. Wu (2014), Influences of soil moisture and vegetation on convective precipitation forecasts over the United States Great Plains, *J. Geophys. Res. Atmos.*, *119*, 9338–9358, doi:10.1002/2014JD021454.

Received 3 JAN 2014
Accepted 11 JUL 2014
Accepted article online 14 JUL 2014
Published online 7 AUG 2014

Influences of soil moisture and vegetation on convective precipitation forecasts over the United States Great Plains

Thomas W. Collow[1,2], Alan Robock[1], and Wei Wu[3]

[1]Department of Environmental Sciences, Rutgers University, New Brunswick, New Jersey, USA, [2]Now at INNOVIM, LLC., NOAA/NWS/NCEP/Climate Prediction Center, College Park, Maryland, USA, [3]Environmental and Climate Sciences Department, Brookhaven National Laboratory, Upton, New York, USA

Abstract This study investigates the influences of soil moisture and vegetation on 30 h convective precipitation forecasts using the Weather Research and Forecasting model over the United States Great Plains with explicit treatment of convection. North American Regional Reanalysis (NARR) data were used as initial and boundary conditions. We also used an adjusted soil moisture (uniformly adding 0.10 m^3/m^3 over all soil layers based on NARR biases) to determine whether using a simple observationally based adjustment of soil moisture forcing would provide more accurate simulations and how the soil moisture addition would impact meteorological parameters for different vegetation types. Current and extreme (forest and barren) land covers were examined. Compared to the current vegetation cover, the complete removal of vegetation produced substantially less precipitation, while conversion to forest led to small differences in precipitation. Adding 0.10 m^3/m^3 to the soil moisture with the current vegetation cover lowered the near surface temperature and increased the humidity to a similar degree as using a fully forested domain with no soil moisture adjustment. However, these temperature and humidity effects on convective available potential energy and moist enthalpy nearly canceled each other out, resulting in a limited precipitation response. Although no substantial changes in precipitation forecasts were found using the adjusted soil moisture, the similarity found between temperature and humidity forecasts using the increased soil moisture and those with a forested domain highlights the sensitivity of the model to soil moisture changes, reinforcing the need for accurate soil moisture initialization in numerical weather forecasting models.

1. Introduction

Land surface vegetation exchanges energy, water vapor, and various gases with the surrounding environment (soil and atmosphere) and thus influences atmospheric variables such as temperature, humidity, and precipitation. Accurate simulations of land surface-atmosphere interactions are critical to most regional or global climate and weather forecast models. This study investigates the sensitivity of convective precipitation forecasts to vegetation and soil moisture using the Weather Research and Forecasting (WRF) model on a short time scale over the United States Great Plains, which has been noted by *Koster et al*. [2006] as a "hot spot" for land-atmosphere coupling. The major focus of this study is on the total amount of precipitation but not on its location and occurrence.

Many previous studies have focused on the relationship between vegetation cover and weather patterns. For example, *Blyth et al*. [1994] found a 30% increase in precipitation when their model was run using a pure forested landscape compared to a completely bare landscape over France. Other vegetation impact studies by *Raddatz* [1998], *Doran and Zhong* [2000], *Weaver and Avissar* [2001], *Gero et al*. [2006], *Matyas and Carleton* [2009], and *Hong et al*. [2009] all found some interaction between vegetation and convective development. *Yu et al*. [2012] used the WRF model and found increases in precipitation and decreases in temperatures over a 10 year period when switching barren land with grassland to simulate regrowth of vegetation in northern China. *Trail et al*. [2013] did not find any meaningful precipitation changes as a result of changing cropland to forested land across the southeastern United States but did note an effect on temperatures. *Bollasina and Nigam* [2011] conducted a 1 year simulation, also using the WRF model, in which the desert land of northwestern India and Pakistan was expanded by a factor of 9, which resulted in local precipitation decreases. A conversion from urban land to natural land diminished thunderstorm development over

Sydney, Australia [*Gero et al*., 2006]. Further research by *Ashley et al*. [2011] concluded that there was a higher frequency and intensity of thunderstorms over the major urban areas investigated over the southeastern United States. Although removal of vegetation usually creates less precipitation, as seen in many studies, conversion to urbanized land can produce higher surface air temperatures, which can motivate additional vertical convection [*Comarazamy et al*., 2010, 2013]. This study will not focus on urban development, making the reduced convection scenario more feasible as a result of vegetation removal.

Several studies also found strong relationships between soil moisture and precipitation. For example, *Eltahir* [1998] provided a pathway which suggested a positive feedback between soil moisture and precipitation. *Evans et al*. [2011] credited anomalously high soil moisture as the primary reasoning behind the reintensification of Tropical Storm Erin over Oklahoma in 2008. They conducted simulations with lower initialized soil moisture, which resulted in a weaker cyclone. *Pielke and Zeng* [1989] found that the lifted index, or the temperature difference between the 500 mb environmental temperature and the temperature of an adiabatically lifted air parcel at the same level (environmental temperature minus parcel temperature), was much less over irrigated land than over dry land, signifying a greater chance for thunderstorm development over wetter soils. While the aforementioned studies all showed increased soil moisture resulting in more precipitation, several others have shown the opposite relationship. Work by *Taylor and Ellis* [2006] supports a negative feedback between soil moisture and precipitation as they found suppressed cold cloud development within regions of wet soil over the Sahel region of Africa. On a much larger scale, *Taylor et al*. [2012] determined that afternoon convection was maximized over drier soils over most of the globe using observations. The study also highlighted the performance of several climate models which tend to incorrectly favor precipitation over wet soils. *Taylor et al*. [2013] pointed out the limited ability of climate models to accurately parameterize convection and showed that using explicit treatment of convection resulted in the generation of convection over drier soils which agreed more with observed data, as opposed to parameterized convection which favored convection over wet soils. Because *Taylor et al*. [2013] focused over the Sahel, more studies of this nature are needed across the world, which utilize an explicit treatment of convection.

Soil moisture can affect convective precipitation in two basic ways. Increased soil moisture enhances evapotranspiration, cooling the surface but at the same time adding more moisture to the atmosphere. Cooling would tend to reduce convection, and thus reduce precipitation, but the added moisture would enhance precipitation. *DeAngelis et al*. [2010], in a study of increased irrigation in the United States Great Plains, found that locally the two impacts of wetter soil canceled each other out, producing no impacts on precipitation. Downwind however in the United States Midwest, precipitation was higher with increasing Great Plains irrigation because of the increase in advected water vapor. Additional studies showed that soil moisture change induced by dam construction had an impact on extreme precipitation [*Hossain et al*., 2009], specifically over northern California [*Woldemichael et al*., 2012] and eastern Oregon [*Woldemichael et al*., 2014]. *Degu et al*. [2011] also showed that the largest effects of this were across the western United States, and noted a less apparent relationship in more humid climates such as the Great Plains, which adds to the overall uncertainty of the soil moisture-precipitation relationship. In this study we examine how changes in soil moisture impact precipitation, temperature, and humidity with a focus on cases of severe weather outbreaks and strong convection exclusively over the Great Plains.

Another unresolved question is whether the impacts of soil moisture on convection depend on surface vegetation. While there has been a great deal of work individually on studying the sensitivity of precipitation to either soil moisture or vegetation changes, there is a limited amount of literature on changing both concurrently. *Wang et al*. [2006] noted that anomalies in the normalized difference vegetation index in spring had a statistically significant effect on temperatures and precipitation in late summer due to vegetation controlling the amount of soil moisture at the surface, with positive vegetation anomalies depleting more soil moisture over time and vice versa. *Clark and Arritt* [1995] developed a primitive single-column model and found that convection was maximized with increased vegetation and soil moisture. *Mahmood et al*. [2011] performed a series of modeling experiments using the National Center for Atmospheric Research (NCAR) Fifth Generation Mesoscale Model over a small area in western Kentucky, which investigated the relationship between soil moisture, greenness fraction, and land use type. They found a relationship among all three variables, with soil moisture changes moderating those imposed by vegetation changes. *De Ridder* [1997] studied the influence of land surface on thermodynamic potential for deep convection using a one-dimensional column model, finding that the potential for moist convection increased with evaporative fraction.

In a subsequent study, *De Ridder* [1998] coupled a single-column model to a land surface model to analyze land surface-atmosphere interactions over the West African Sahel. This last study showed that infiltrated rainwater remained available for evaporation much longer on a vegetated surface than on a bare soil surface providing evidence of a positive feedback between increased vegetation and convection. *Kim and Wang* [2007a] discovered that precipitation increased linearly as soil moisture increases were imposed in a certain range. The work was expanded by *Kim and Wang* [2007b] to look into the vegetation-precipitation feedback, and their results showed that vegetation enhanced the soil moisture precipitation feedback. Because the work was done using a climate model with $2° \times 2.5°$ horizontal grid spacing, concluding remarks called for simulations using finer grid spacing to address feedbacks at a scale suitable for convection. *Hong et al*. [2009] experimented with soil moisture and vegetation interactions using WRF runs with small grid spacing to analyze both factors; however, they did not reach a definitive conclusion regarding the soil moisture sensitivity of the model.

Current weather forecasting models are forced with soil moisture that may not necessarily be accurate, which may lead to errors in their ability to forecast. Surface temperatures are sensitive to soil moisture with the 2003 European summer heat wave as a good example. As explained by *Fischer et al*. [2007], summer temperatures in Europe exceeded the 1961–1990 mean by about 3°C over large areas and by over 5°C regionally. They found that there was a strong precipitation deficit in the early part of that year leading to drier than normal soils. Their experiments proved that soil moisture played a significant role in the warmer temperatures, as when model simulations using climatological mean soil moisture values were conducted, the resultant temperature anomalies were reduced by 40%. Therefore, this study proposes to apply a simple adjustment to soil moisture in the North American Regional Reanalysis (NARR) [*Mesinger et al*., 2006] data set used to force the WRF model and compare the resulting changes in the model simulations to those that would be found by imposing extreme changes in vegetation. Not only will this provide insight into whether or not corrected soil moisture would result in better weather forecasts of strong convection, but it will also allow for an analysis of the effects of altering both soil moisture and vegetation over a large domain. This study is different from others in that it is looking purely into the relationship between soil moisture, vegetation, and precipitation at a large scale by using a small enough horizontal grid spacing to model convection explicitly, while ignoring the effects of gradients by imposing uniform changes. In addition, this study aims to provide insight into the NARR soil moisture data and compare the results to observations to determine if the soil moisture addition can result in any improvements in the forecasts of temperature, humidity, and precipitation. Due to climate change and increased land development, changes will occur to both the vegetation and the soil moisture concurrently, and it is necessary to understand how they will both interact rather than focusing on these factors individually.

2. Data and Methods

2.1. Model Configuration

We used version 3.4.1 of the Advanced Research WRF core [*Skamarock et al*., 2008], which was the newest, most up-to-date version of WRF available at the onset of the study. Our standard configuration of the WRF model (choices of parameterization schemes) was designed to closely match that used by the National Oceanic and Atmospheric Administration Storm Prediction Center (SPC), since our primary focus was on mesoscale convective events. This configuration was also used by *Case et al*. [2011], who investigated convective forecasts using the improved soil moisture data from a land surface model using small grid intervals. For microphysics, the WRF single-moment 6-class scheme [*Hong and Lim*, 2006] was employed. This scheme added information on the graupel mixing ratio in addition to the already present mixing ratios of water vapor, cloud water, cloud ice, rain, and snow found in previous versions of the scheme. The Rapid Radiative Transfer Model [*Mlawer et al*., 1997] was used for longwave radiation, and the Dudhia scheme [*Dudhia*, 1989] was implemented for shortwave radiation. The longwave scheme accounts for the various absorption properties of common atmospheric constituents including ozone, water vapor, and carbon dioxide. The shortwave scheme is governed by the solar zenith angle, which affects the path length of radiation originating from the Sun. It also uses information on clouds which have an albedo and absorption properties, in addition to clear air conditions where there can still be water vapor absorption of radiation as well as scattering. For the planetary boundary layer (PBL), the Mellor-Yamada-Janjic (MYJ) scheme [*Mellor and Yamada*, 1982], which includes prognostic calculations of turbulent kinetic energy, was used. It is also the operational scheme in the North American Mesoscale model. In addition, the WRF model was coupled to the Noah Land Surface Model [*Ek et al*., 2003].

Table 1. Areal Mean Total Precipitation (mm) From 18 UTC 10 May 2010 Through 06 UTC 11 May 2010 From WRF Runs With Different Configurations[a]

Scheme Combination	Control Vegetation Inner|Outer	Forested Vegetation Inner|Outer	Barren Vegetation Inner|Outer
WSM6-MYJ	2.59|4.41	3.83|4.67	1.05|3.72
WSM6-Yonsei	2.49|4.63	4.20|5.09	1.18|3.94
WSM6-QNSE	2.74|4.58	3.57|4.79	0.92|3.70
Goddard-MYJ	1.63|4.26	2.88|4.27	0.67|3.36
Goddard-Yonsei	1.46|3.99	2.65|4.69	0.60|3.53
WSM6-MYJ + 0.10 soil moisture (SM)	2.77|4.46	4.28|4.90	1.10|3.94

[a]The left number represents the inner domain and the right number represents the outer domain, which are both presented in Figure 3. For reference, the areal mean precipitation from the NCEP observations across the inner and outer domains was 6.17 mm and 4.57 mm, respectively.

For two of the cases, a five-member ensemble of runs was conducted using different microphysics and boundary layer schemes to address the issue of model variability, a method employed by the Short-Range Ensemble Forecasting System [*Charles and Colle*, 2009] and noted by *Stensrud et al.* [2000] as a good method for creating model ensembles. The Goddard Microphysics scheme [*Tao and Simpson*, 1993] was used as well as the Yonsei University [*Hong et al.*, 2006] and Quasi-Normal Scale Elimination (QNSE) [*Sukoriansky et al.*, 2005] PBL schemes. Although there are many options for different schemes to use, many of the schemes were eliminated as candidates, because they are inappropriate for studies using small grid separation, too computationally expensive, or have not been tested adequately. The specific pairings of microphysics and boundary layer schemes are listed in Tables 1 and 2. The same set of initial conditions was used for each configuration.

The model domains were set up as follows. The WRF preprocessing system (WPS) was set up with an outer domain with a 36 km horizontal grid increment covering a 130 × 82 (*x-y*) grid (Figure 1). The first nest used a 12 km horizontal grid increment and covered a 274 × 181 grid. Finally, the second nest, which generated the output analyzed in this study, was at a 4 km horizontal grid increment and contained a 429 × 336 grid. The innermost nest had a small enough grid spacing for convection to be treated explicitly. *Kain et al.* [2008] determined that a decrease to a 2 km horizontal grid increment would provide greater detail but not improve the overall skill of the model to produce convection. We ran simulations (not shown) with a 1.3 km horizontal grid increment and found no improvement over the 4 km runs. Because of the high computational demands of such runs, we decided to use a 4 km horizontal grid increment for this study. All nests were centered over the United States Great Plains and contained 29 vertical levels, starting at 1000 mb and decreasing by 25 mb until 700 mb. Then the levels decrease by 50 mb until reaching 300 mb, where they decrease by 25 mb again before stopping at the top layer, which is 100 mb. All runs used data from NARR as initial and boundary conditions. NARR directly assimilates observed precipitation and radiances and uses the Noah Land Surface Model, the same land surface model being used in the WRF simulations for this experiment. Five events were chosen with strong synoptic forcing for convection, as explained in section 2.3. Each run was initialized at 00 UTC and terminated at 06 UTC the next day. Analysis began after 18 h.

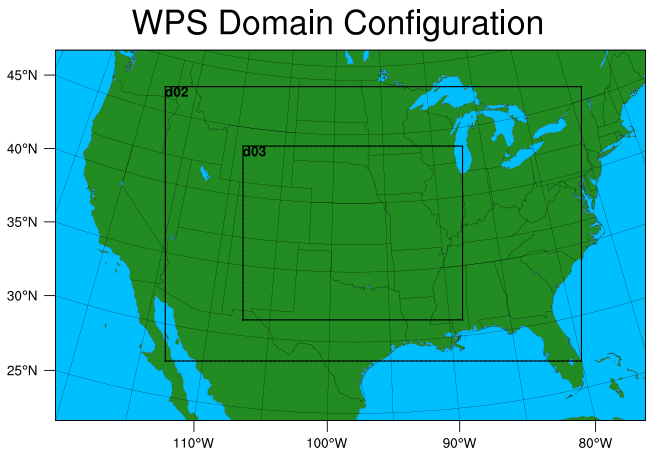

Figure 1. Domain nests used for WRF experiments generated by the WPS. Outer domain (the entire image) was nudged at the edge by the NARR data and run at a grid increment of 36 km. Domain d02 was run at 12 km grid increment. Results shown in paper are for the inner domain, d03, run at a 4 km grid increment.

2.2. Soil Moisture and Vegetation

The following runs were performed to analyze land surface effects on the atmosphere. First, a control run was performed using current land use and

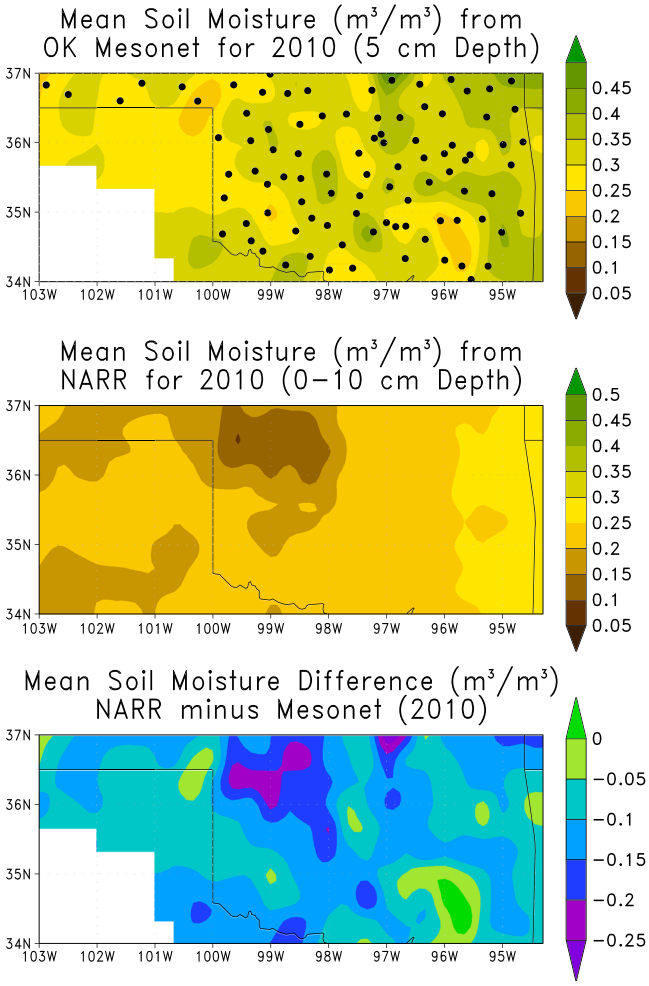

Figure 2. Mean volumetric soil moisture (m^3/m^3) from (top) the Oklahoma Mesonet for 2010, (middle) the mean soil moisture from NARR, and (bottom) the difference between NARR and Mesonet. Oklahoma Mesonet stations are plotted in Figure 2 (top).

NARR soil moisture. Runs with adjusted soil moisture were then conducted. A uniform addition of 0.10 m^3/m^3 volumetric was added to the original NARR soil moisture, based on comparisons to in situ observations from the Oklahoma Mesonet during 2010 (Figure 2), rather than a percent increase, which would strengthen soil moisture gradients and therefore have an effect on precipitation independent from the vegetation interactions [*Chang and Wetzel*, 1991; *Taylor et al.*, 2011; *Suarez et al.*, 2014]. It was assumed that the soil moisture bias was valid for the entire d03 domain, although it was difficult to fully assess due to the lack of available soil moisture observations. This simple adjustment was made at all depths of soil to preserve vertical gradients as well. The Noah Land Surface Model contains four soil moisture levels, namely, 0–10 cm below the surface, 10–40 cm below, 40–100 cm below, and 100–200 cm below. The upper bound of soil moisture was set to the porosity. Studies such as *Richter et al.* [2004] and *Guillod et al.* [2013] have noted the importance of having correct soil moisture parameters, such as soil texture, in numerical models. Since the same land surface model was used in our experiment and in NARR (Noah), soil properties remained constant, and thereby, soil moisture range and biases were likely similar, making our experimental design appropriate. Initial soil moisture perturbations in the model persisted throughout the entire run as the time frame of the simulations (30 h) was too short compared to the time scale of soil moisture variations (1–3 months [*Vinnikov et al.*, 1996; *Entin et al.*, 2000; *Nie et al.*, 2008]).

Soil moisture changes were then tested on different vegetation configurations in an effort to better understand the vegetation-soil moisture relationship in the WRF model. Vegetation type was changed to both "evergreen broadleaf forest" and "barren or sparsely vegetated" across the entire d03 domain with appropriate adjustments in albedo and greenness fraction. Although several studies [*Crawford et al.*, 2001; *Kurkowski et al.*, 2003; *Hong et al.*, 2009; *James et al.*, 2009; *Sertel et al.*, 2010; *Case et al.*, 2012; *Kumar et al.*, 2013] have worked to adjust a model's original vegetation scheme to provide a greater level of detail, using the original data set was suitable for this study since comparisons were only being made with extreme vegetation cover scenarios. Vegetation changes and soil moisture changes were independent of each other in the present study with the vegetation changes not impacting soil moisture at the initial time. While model spin-up is important, especially for vegetation changes, this work did not perform any early spin-up because the results were easier to assess if only one variable was changed for each simulation rather than a spin-up scenario which would impact both soil moisture and vegetation simultaneously. Although this may have created unrealistic scenarios as any vegetation change would likely have some impact on soil moisture, the advantage here was that the modeled changes in precipitation, temperature, or dewpoint were able to be directly linked to either changes in soil moisture or changes in vegetation.

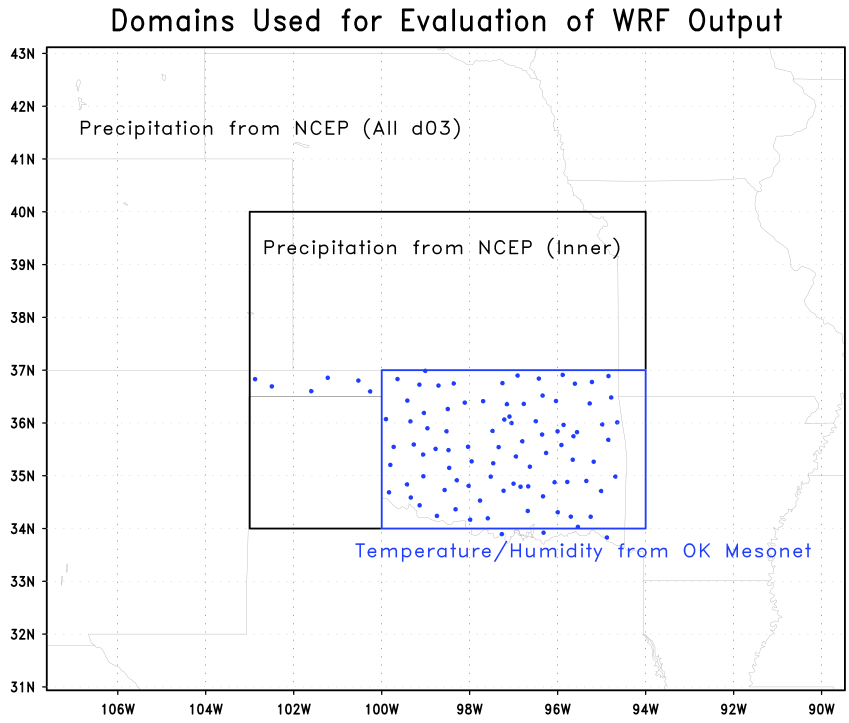

Figure 3. Map showing the different domains used for evaluation throughout this paper. Precipitation is evaluated against the NCEP Stage IV data across the entire d03 domain as well as in an inner region including Oklahoma and Kansas. Surface parameters of temperature and humidity are compared to Oklahoma Mesonet observations (the panhandle was excluded to maintain a uniform boxed region with a dense set of observations). The locations of the Mesonet sites are marked in blue for reference.

2.3. Cases

The SPC has issued a high risk for severe weather for five cases over the Southern Great Plains since 2009, and these were chosen as candidates for this study, namely, 26 April 2009, 10 May 2010, 19 May 2010, 27 May 2011, and 14 April 2012. The high-risk designation from the SPC is only used a few times per year and denotes the likelihood for extreme severe weather, including violent tornadoes and high-wind events (http://www.spc.noaa.gov/misc/about.html). Each of these cases includes a low-level jet stream bringing copious amounts of moisture from the Gulf of Mexico region along with a dryline, bringing in very dry air from the Western U.S., creating a highly favorable environment for thunderstorm development.

Precipitation patterns were compared for each land surface scheme, as well as changes in 2 m temperature and humidity. We focused on these parameters as they are important determinants of convective evolution. We evaluated precipitation over two domains, the entire d03 domain from Figure 1 (outer) and an inner domain encompassing Oklahoma and Kansas (Figure 3) using the National Centers for Environmental Prediction (NCEP) Stage IV Product. This product is available at a 4 km horizontal grid increment, the same as the innermost grid increment used in this study. It was derived from both radar and gauge data and underwent some degree of quality control [*Lin and Mitchell*, 2005]. Although the inner domain is arbitrary, it was used because it was the primary region for convective development, while the areas outside this region received more nonconvective precipitation. Modeled temperature and relative humidity were evaluated against observations from the Oklahoma Mesonet over the main region of Oklahoma (see blue box on Figure 3; panhandle excluded to allow for a boxed domain).

3. Results

3.1. Ensemble Analysis

By using five-member ensembles constructed with different parameterization choices for the 10 May 2010 case and the 19 May 2010 case, we found that the model was more sensitive to extreme vegetation removal

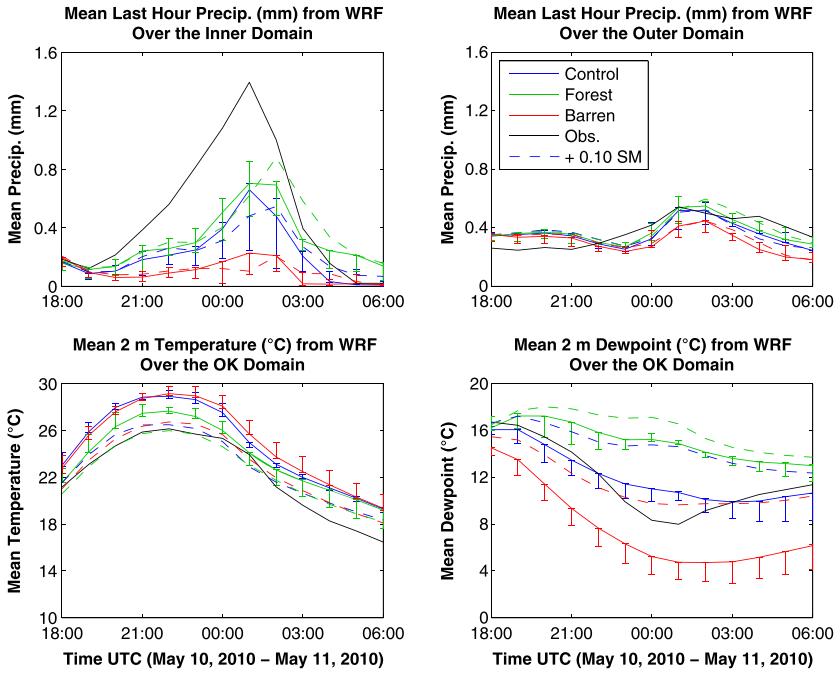

Figure 4. Time series of areal mean hourly precipitation (mm) across (top left) the inner evaluation domain and (top right) the outer domain for the WRF base configuration for different vegetation and soil moisture configurations for the 10 May 2010 case. Also plotted are the corresponding time series for (bottom left) the 2 m temperature and (bottom right) the 2 m dewpoint over the OK domain. Observations for the precipitation plots are from the NCEP Stage IV product and from the Oklahoma Mesonet for the temperature and dewpoint plots. The error bars represent the spread between the minimum and maximum values among the five-member ensemble.

than to using different parameterization choices. Changes to the initial soil moisture resulted in modest variability in precipitation. Although there were five cases to choose from, these two were selected for the ensembles due to their close proximity in time to each other and a similar synoptic setup. Both cases featured a low-pressure system moving through western sections of Oklahoma and Kansas, while a low-level jet stream transported large amounts of moisture into the region. Explosive convection developed on both days leading to numerous severe weather reports including tornadoes. Figures 4 and 5 show a time series of the mean hourly precipitation from the base configuration across the two domains for 10 May 2010 and 19 May 2010, respectively, with the error bars representing the minimum and maximum value at the time among the five different configurations. Total precipitation amounts from the individual ensembles are provided in Tables 1 (10 May) and 2 (19 May). The base WRF run with control vegetation and soil moisture had too little precipitation for the 10 May 2010 case and was too wet for the 19 May 2010 case when compared to the NCEP observations. Using the Goddard Microphysics scheme produced less precipitation on both days in the WRF control vegetation simulation. This was the least accurate scheme on 10 May 2010, since the observed precipitation exceeded the modeled precipitation but performed better on 19 May 2010 due to less precipitation in the observations than in the model.

It is also evident from the figures that the barren land cover is significantly drier than both the forested land cover and the control land cover; however, there is no substantial difference between the control land cover and the forested land cover. Adding soil moisture to the base configuration did not result in significant differences relative to the ensembles, showing that the soil moisture adjustment did not significantly change precipitation forecasts as the changes were similar to or smaller than the changes that resulted from changing the model's internal configuration. Also plotted in Figures 4 and 5 are the mean 2 m temperature and 2 m dewpoint for the two cases over the Oklahoma domain (to allow comparison to Oklahoma Mesonet data). Soil moisture changes have a large cooling effect on temperature in both cases, more so than vegetation changes. The error bars extend low on both dewpoint plots signifying lower dewpoints in the ensembles than from the base configuration likely

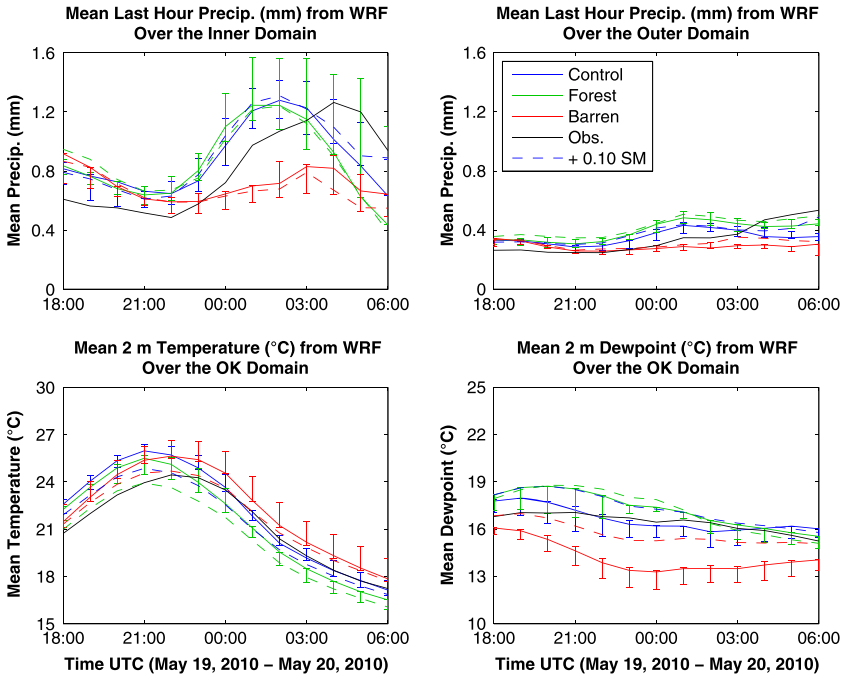

Figure 5. Same as Figure 4 except for the 19 May 2010 case.

due to better treatment of entrainment processes in the Yonsei University boundary layer scheme, allowing for a faster progression of the dryline. Both vegetation and soil moisture result in fairly robust dewpoint changes. The mechanisms in which these temperature and dewpoint responses impact precipitation are discussed in more detail in section 4.

Another method of analyzing precipitation comes not just from looking at spatial means but from looking at the spatial frequency of precipitation amounts. Figure 6 shows a time series of the number of model grid cells above a certain threshold for the 19 May 2010 case with the base configuration. The error bars are constructed the same way as in the previous figure. The plots show similar results with no significant change in precipitation resulting from changing soil moisture. Soil moisture impacts the 0.25 mm threshold the most while not affecting the other two bins as much. This suggests that while the soil moisture changes may play a role in enhancing small precipitation amounts, the fraction of higher amounts is nearly the same. The same pattern was evident on 10 May 2010 to an extent (not shown). However, there was much more variability among the ensembles regarding the amounts greater than 20 mm, making it impossible to draw conclusions from that case. Based on the work done with the parameterization ensembles, it is appropriate to conclude that overall, the soil moisture increases do not impact the WRF modeled precipitation any more than changing the internal configuration of the model. In addition, changes that result from soil moisture alterations are mostly on smaller amounts of precipitation rather than higher amounts of precipitation which

Table 2. Same as Table 1 Except for 18 UTC 19 May 2010 Through 06 UTC 20 May 2010[a]

Scheme Combination	Control Vegetation Inner|Outer	Forested Vegetation Inner|Outer	Barren Vegetation Inner|Outer
WSM6-MYJ	10.78|4.36	10.28|4.92	8.41|3.53
WSM6-Yonsei	12.09|4.50	13.32|5.21	8.37|3.36
WSM6-QNSE	11.39|4.54	11.98|4.86	7.76|3.48
Goddard-MYJ	9.84|4.11	9.77|4.67	7.04|3.37
Goddard-Yonsei	10.80|4.03	12.85|4.87	8.17|3.30
WSM6-MYJ + 0.10 SM	11.20|4.72	10.21|5.31	7.94|3.79

[a]For reference, the areal mean precipitation from NCEP observations across the inner and outer domains was 9.98 mm and 4.16 mm, respectively.

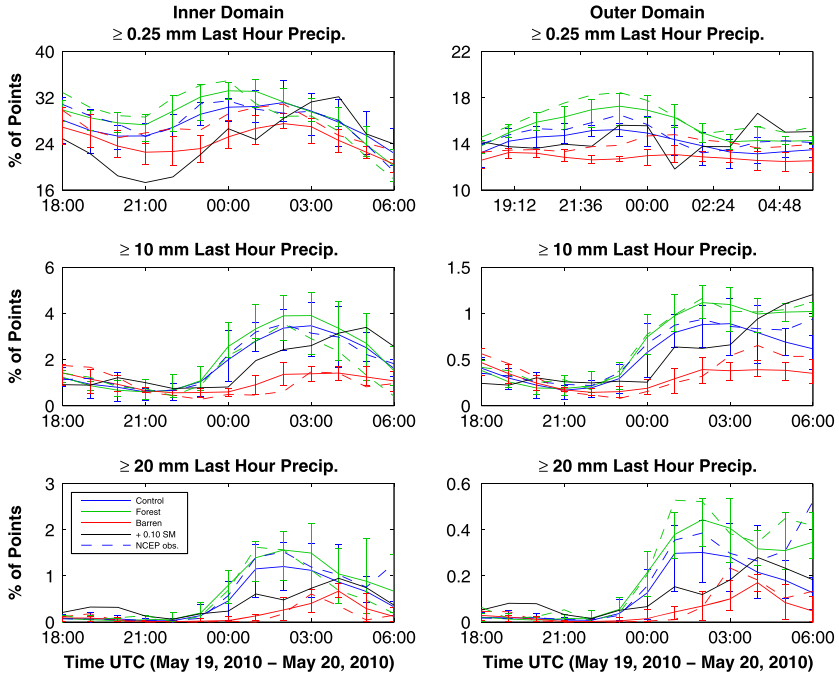

Figure 6. Time series showing the percentage of the WRF grid points above a certain precipitation threshold for the WRF base configuration (solid lines) for (left column) the inner domain and (right column) the outer domain for the 19 May 2010 case. As in Figure 4, the error bars represent the minimum and maximum values from the five-member ensemble. The dotted line represents the adding of 0.10 m^3/m^3 soil moisture to the base configuration. The top, middle, and bottom rows represent the percentage of WRF grid cells with last hour precipitation greater than or equal to 0.25 mm, 10 mm, and 20 mm, respectively.

are more associated with convection. There is no indication that any particular combination of schemes resulted in better forecasts when compared to observations. Therefore, the remaining cases will only use our WRF base configuration as this is a well-tested combination of schemes, although *Coniglio et al.* [2013] found that newer planetary boundary layer schemes such as the Mellor-Yamada-Nakanishi-Niino scheme may be more adequate for use in convection allowing configurations of WRF. The goal will be to continue to analyze the relationship between soil moisture, vegetation, and precipitation and to determine whether or not the same precipitation patterns are seen. In addition, we will look into the 2 m temperature and humidity fields.

3.2. The 26 April 2009 Outbreak

For the 26 April 2009 severe outbreak, the bulk of activity was centered over Kansas. Although tornado reports were minimal, there were many instances of high winds and large hail. The WRF model simulated the development of convection well over Kansas but overestimated the intensity farther south in all of the runs. Figure 7 shows the time series of hourly precipitation from this and the remaining two cases. The control run produced mean total precipitation over the inner domain of 13.16 mm and was 13.88 mm according to the NCEP observations. Mean inner domain total precipitation increased to 14.29 mm for a forested domain and decreased to 10.49 mm for a barren domain. Adding 0.10 m^3/m^3 to soil moisture had minimal effects. Soil moisture had more of an impact when the outer domain was considered, but the impacts were still smaller compared to vegetation changes. For the control case, mean total precipitation within the outer domain increased from 5.78 mm to 6.14 mm due to the increase in soil moisture. For the forested domain, the increase was from 6.66 mm to 6.80 mm and from 4.91 mm to 5.15 mm for the barren land surface. All mean total precipitation values for this and the other cases can be found in Tables 3 and 4 for the inner and outer domain, respectively.

We compared the modeled fields of temperature and dewpoint against the observations from the Oklahoma Mesonet. Between 18 UTC 26 April and 06 UTC 27 April, the mean 2 m temperature over the Oklahoma

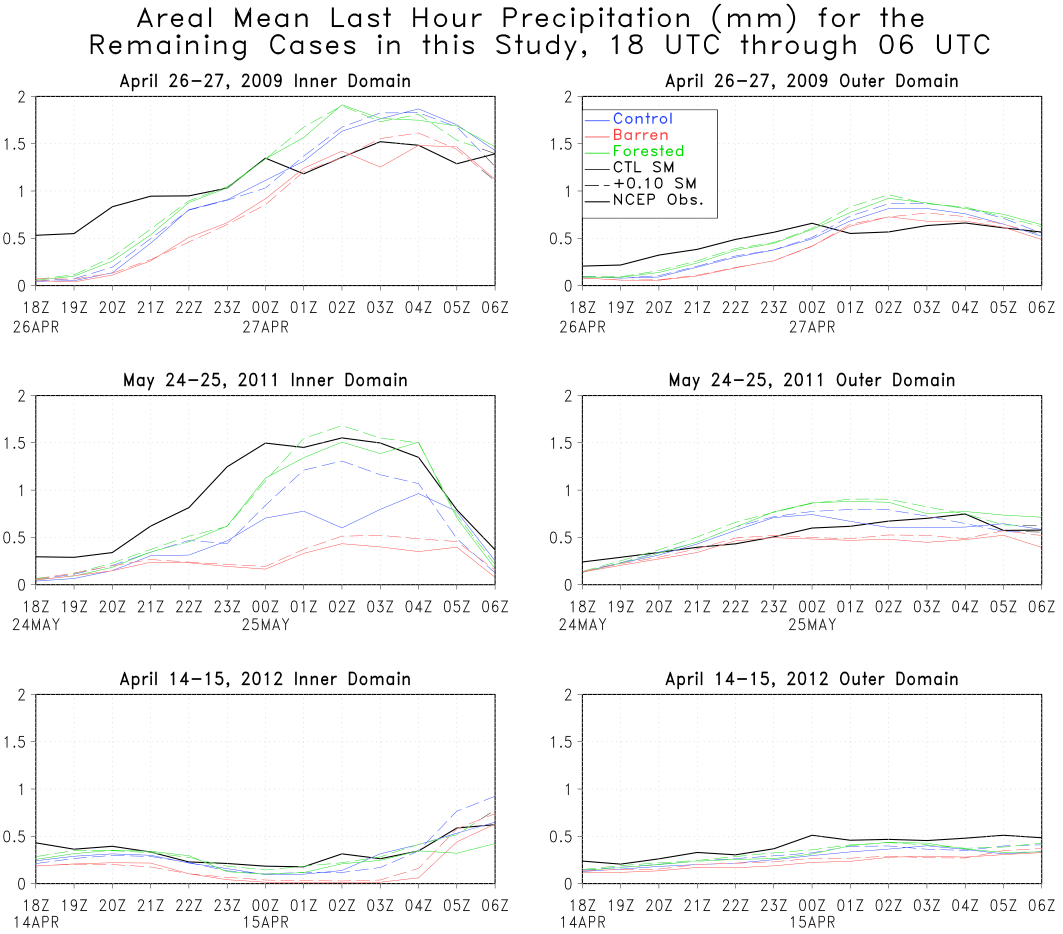

Figure 7. Time series of the areal mean last hour precipitation (mm) from the remaining three cases featured in this study. The inner domain means are in the left column with the outer domain means in the right column. The top, middle, and bottom rows represent the 26 and 27 April 2009, 24 and 25 May 2011, and 14 and 15 April 2012 cases, respectively. The solid lines denote the control soil moisture, and the dashed lines represent the 0.10 m^3/m^3 soil moisture addition.

evaluation domain was 21.6°C. This was cooler than the mean of the Oklahoma Mesonet observations, which was 22.5°C. Therefore, the control mean anomaly was −0.9°C. The anomaly decreased to −2.0°C when 0.10 m^3/m^3 soil moisture was added and to −1.7°C when the land was converted to a forest. Barren land increased the temperature anomaly slightly to −0.8°C. Adding soil moisture had the smallest effect on the completely forested domain with a decrease in temperature of −0.6°C. For the control and barren cases, the decrease was larger, −1.1°C.

Table 3. Areal Mean Total Precipitation (mm) for All the Cases for Each Vegetation and Soil Moisture Configuration Across the Inner Domain From Figure 3[a]

Cases	Control Vegetation |+0.10	Forested Vegetation |+0.10	Barren Vegetation |+0.10	NCEP Observations
26 and 27 April 2009	13.16|13.12	14.29|14.34	10.49|10.71	13.88
10 and 11 May 2010	2.59|2.77	3.83|4.28	1.05|1.10	6.17
19 and 20 May 2010	10.78|11.20	10.28|10.21	8.41|7.94	9.98
24 and 25 May 2011	6.16|7.76	9.44|10.11	3.06|3.74	11.81
14 and 15 April 2012	3.52|3.75	3.19 | 4.03	1.97|2.37	4.03

[a]The base WRF configuration scheme is used. The number on the left is for the run with no soil moisture change and the right for the run with 0.10 m^3/m^3 added to the soil moisture (indicated as +0.10). Time is from 18 UTC, the first day through 06 UTC the next day.

Table 4. Same as Table 3 Except for the Outer Domain From Figure 3

Cases	Control Vegetation |+0.10	Forested Vegetation |+0.10	Barren Vegetation |+0.10	NCEP Observations
26 and 27 April 2009	5.78|6.14	6.66|6.80	4.91|5.15	6.22
10 and 11 May 2010	4.41|4.46	4.67|4.90	3.72|3.94	4.57
19 and 20 May 2010	4.36|4.72	4.92|5.31	3.53|3.79	4.16
24 and 25 May 2011	6.71|7.21	7.98|8.05	5.05|5.51	6.45
14 and 15 April 2012	3.42|3.81	3.74|4.06	2.72|3.04	4.84

For determining humidity relationships, the mean 2 m dewpoint between 18 UTC and 06 UTC the next day is used. Figure 8 highlights the maximum progression of the 10°C isodrosotherm across Oklahoma for each of the cases and land surface configurations. The different vegetation covers produce alterations in dryline behavior, which influence the spatial mean of the dewpoint temperatures independently of the direct relationship to vegetation [*Lanicci et al.*, 1987; *Grasso*, 2000]. For example, a barren land surface tends to push the dryline farther east, which would promote additional drying compared to the control run, while the forested run would result in the dryline staying farther west. Soil moisture additions are not seen to have a major impact on the dryline in this study. The control run produced an areal mean dewpoint of 16.7°C, which agrees closely to the Oklahoma Mesonet which had a mean of 16.4°C. The soil moisture addition increased the mean dewpoint to 17.2°C, while the forested land increased it to 17.4°C. The barren land surface lowered the value to 15.8°C. The soil moisture addition had the largest impact on the barren land and the smallest impact on the forested land with mean dewpoint increases of 0.2°C and 0.8°C for forest and barren, respectively.

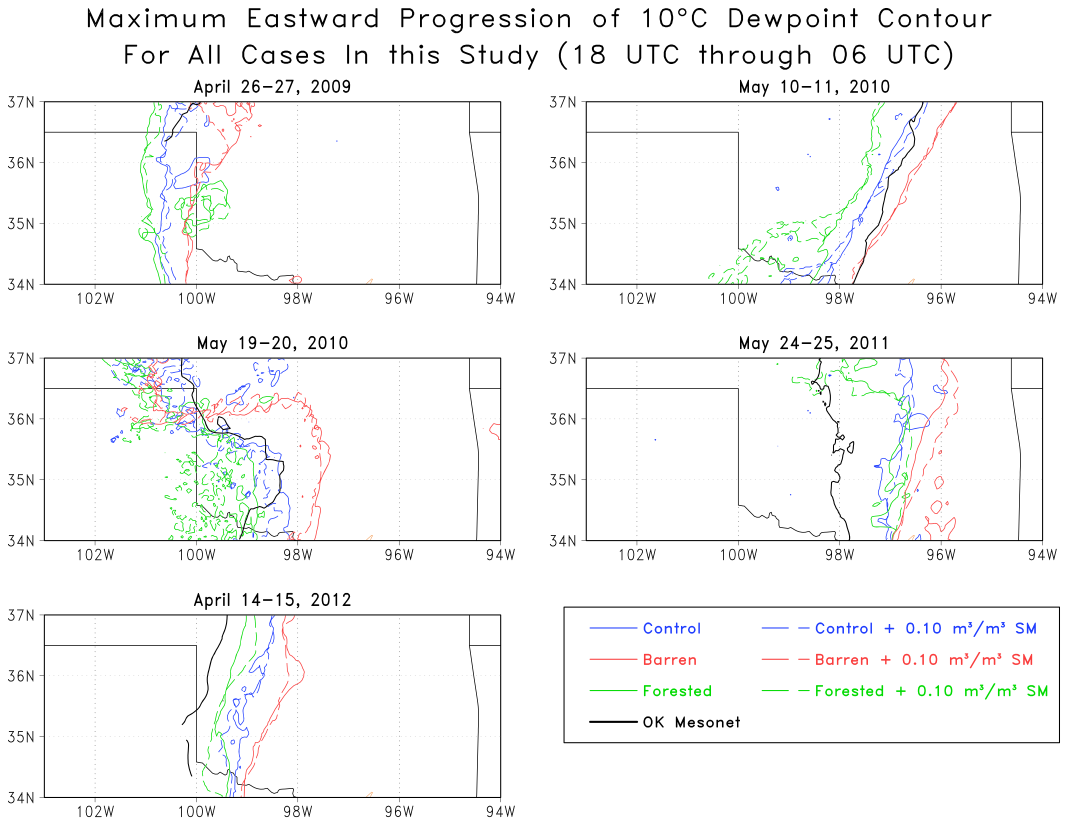

Figure 8. Minimum of the 10°C isodrosotherm for all of the cases signifying the eastward extent of the dryline. Clockwise from top left: 26 and 27 April 2009 case, 10 and 11 May 2010 case, 24 and 25 May 2011 case, 14 and 15 April 2012 case, and 19 and 20 May 2010 case.

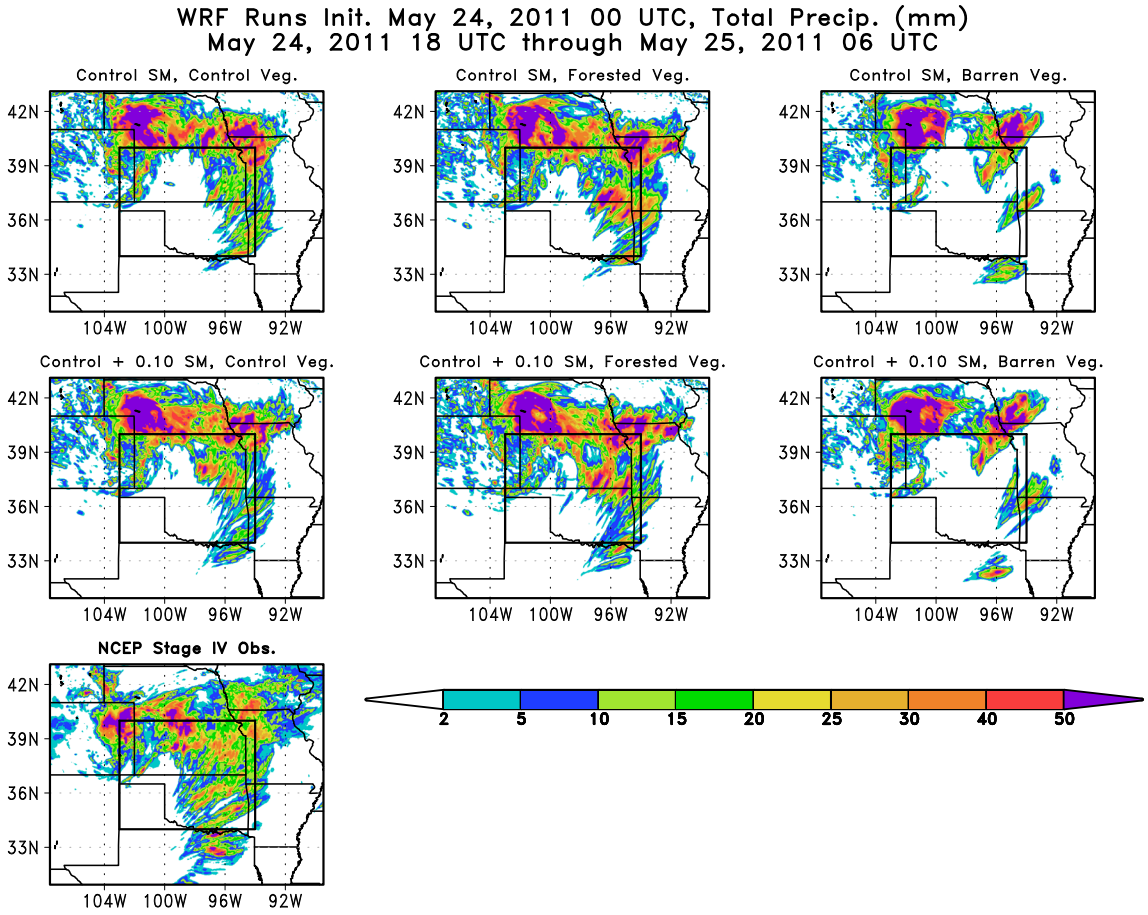

Figure 9. Total precipitation (mm) from 18 UTC 24 May 2011 through 06 UTC 25 May 2011 for different land surface initializations. The top row represents the control NARR soil moisture, and the middle row signifies the 0.10 m^3/m^3 addition. The left, middle, and right columns denote the control, forested, and barren vegetation covers, respectively. (Bottom) Precipitation observations from the NCEP. The black box encloses the inner evaluation domain.

3.3. The 24 May 2011 Outbreak

The 24 May 2011 outbreak was similar in terms of convective development to 10 May and 19 May 2010 but more expansive. The mean value of total precipitation over the inner domain was 6.16 mm. This was still substantially less than the NCEP observations which had an average of 12.11 mm. The forested WRF run produced a mean precipitation of 9.44 mm, and the barren had 3.06 mm. Mean total precipitation over the outer domain was 6.71 mm for the control run, 7.98 mm for the forested, and 5.05 mm for the barren. Adding 0.10 m^3/m^3 to the soil moisture increased the mean total precipitation by 1.60 mm, 0.73 mm, and 0.68 mm over the inner domain for the control, forested, and barren vegetation, respectively. For the outer domain, the increase in soil moisture resulted in mean total precipitation increases of 0.50 mm for the control vegetation, 0.07 mm for the forested, and 0.46 mm for the barren.

The precipitation increases from soil moisture are still less than those from vegetation. Figure 9 shows a spatial map of the total precipitation for this case for all of the land surface configurations. It appears that the control vegetation run using original NARR soil moisture had similar spatial coverage as the increased soil moisture runs but did not capture some of the higher intensities over Oklahoma seen in the increased soil moisture run as well as the forested runs. However, it is clear to see that there is much less precipitation coverage in both barren configurations than the other land covers.

The control simulation produced conditions too warm and dry over Oklahoma compared to the observations. Therefore, the soil moisture addition led to an improvement in both parameters. Specifically, the mean temperature from the control simulation was 32.5°C, and the mean dewpoint was

9.7°C. Adding soil moisture brought the mean temperature down to 30.1°C. This was still too warm compared to the observed value of 28.5°C, but it was still an improvement. The dewpoint increased by 4.0°C when soil moisture was added to the control run but still produced a value less than the observed of 15.5°C. In Figure 8, it is evident that the dryline propagated much farther east in the model than in the observations which would explain the big differences. However, since the soil moisture additions do not appear to impact the dryline significantly, the relationships to the unchanged soil moisture simulations are still pertinent. Adding soil moisture resulted in temperature decreases of 2.4°C for control, 1.6°C for forested, and 1.8°C for barren and dewpoint increases of 4.0°C for control, 2.5°C for forested, and 3.6°C for barren.

3.4. The 14 April 2012 Outbreak

The 14 April 2012 outbreak differs from the others in terms of timing, as most of the convection developed at the end of the model run, which made it more difficult to evaluate. The control vegetation cover produces a mean total precipitation of 3.52 mm over the inner domain. This value decreases to 3.19 mm for the forested domain and further decreases to 1.97 mm for the barren domain. Although the forested domain decreased the precipitation for this case, the addition of soil moisture prompted the largest increase in the mean to 4.03 mm. This was larger than the control vegetation with adjusted soil moisture which had an area precipitation mean of 3.75 mm. The outer domain has areal mean values for total precipitation of 3.42 mm, 3.74 mm, and 2.72 mm for control, forested, and barren vegetation covers, respectively. The soil moisture adjustment increases these values by 0.39 mm for control vegetation and 0.32 mm for both forested and control vegetation.

In this case the modeled temperature was cooler than the observations. Upon adding soil moisture to the control vegetation simulation, the temperature decreased from 22.4°C to 21.5°C, bringing the temperature farther down from the observed value of 23.1°C. Converting to the forest without changing the soil moisture produced a mean temperature of 21.5°C, same as the soil moisture adjusted control run. Adding soil moisture to the forested simulation decreased the mean temperature by 0.4°C. Adjusting the soil moisture in the barren simulation decreased the temperature from 22.7°C to 21.6°C. The control simulation produced a mean dewpoint too low compared to the observations, and adding soil moisture brought it closer into agreement. Specifically, the mean dewpoint increased from 17.0°C in the control run with unchanged soil moisture to 18.0°C with the adjusted soil moisture, which was closer to the observed value of 18.1°C. The forested run with unchanged soil moisture resulted in a mean dewpoint of 18.1°C, identical to the observations and very close to the control run with increased soil moisture. The barren simulation produced a drier mean dewpoint of 15.0°C, and increasing the soil moisture resulted in the value rising to 16.4°C.

4. Discussion

The results showed that a change in the current land surface to a barren land surface created substantially less precipitation, while a change to a forested land surface produced more precipitation in most but not all the cases. However, because the ensemble spread between control and forested vegetation scenarios had a good deal of overlap, it can be concluded that while the drying induced by the barren land configuration was significant, the slight wetting by the forested simulations was not. In the 19 May 2010 case, the forested land surface actually decreased the mean total precipitation with respect to control in some of the ensembles. Overall, results from this study mainly confirm the results of previous studies such as *Bollasina and Nigam* [2011] and *Yu et al.* [2012]. However, it is necessary to consider that this study applied the vegetation changes using small grid spacing. The horizontal grid increments used in the two aforementioned studies were 36 km and 60 km, respectively, while this work used a 4 km horizontal grid increment and focused on convection, which was treated explicitly rather than parameterized.

Generally adjusting the soil moisture upward neither enhanced nor degraded the impacts of vegetation changes on precipitation. This was true for both the inner and outer domains. Because vegetation cover is directly related to evapotranspiration, an increase in soil moisture may be expected to have its maximum impact on precipitation over forested land, because the moisture transport would be maximized [*Clark and Arritt*, 1995]. Mean latent heat fluxes were indeed maximized for the forested simulations with adjusted soil

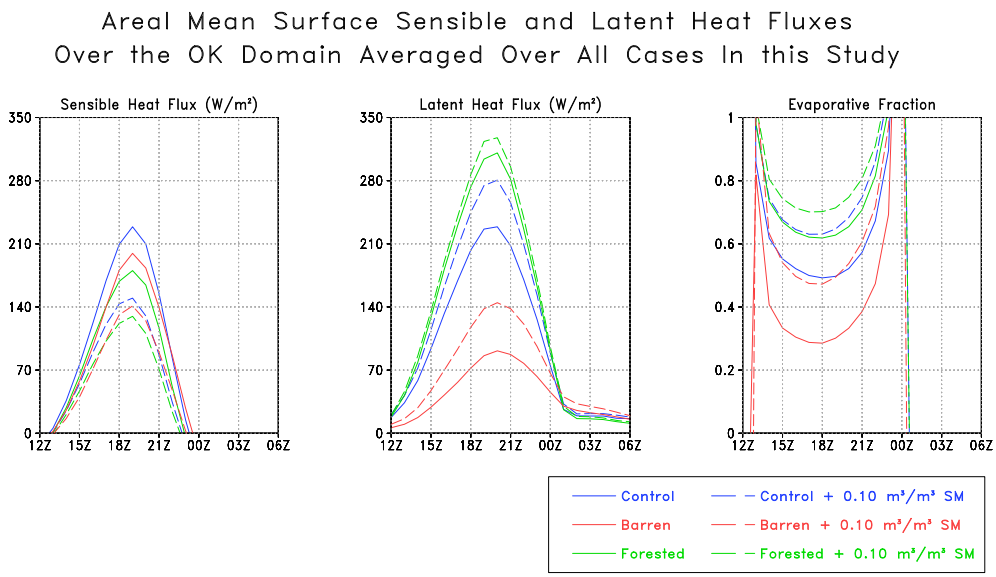

Figure 10. Areal mean of the surface fluxes of (left) sensible heat (W/m^2) and (middle) latent heat (W/m^2) for the different vegetation and soil moisture conditions over the OK domain. All five cases from this study are incorporated into the mean. (right) The evaporative fraction is also plotted.

moisture (Figure 10). Soil moisture impacted the sensible heat fluxes to a greater degree than the vegetation changes, but the vegetation changes had larger effects on latent heat transport. The control vegetation produced the highest sensible heat fluxes due to the forested vegetation resulting in increased shading and the barren land having a higher albedo and reflecting more shortwave radiation. Also shown in Figure 10 is the evaporative fraction, defined as the ratio of the latent heat flux to the sum of the latent and sensible heat fluxes. The evaporative fraction was minimized during the daytime for the barren land scenario with no soil moisture increase. Adjusting the soil moisture in the control run resulted in a nearly identical evaporative fraction to the forested simulation that had no soil moisture change. The evaporative fraction was most affected by soil moisture changes in the barren vegetation simulations and least impacted in the forested vegetation experiments, which would support the fact that the soil moisture adjustment in the forested simulation produced the smallest mean 2 m temperature and dewpoint changes in four out of the five cases. As addressed by *Koster et al.* [2006] and *Kim and Wang* [2007b], the model's soil moisture biases are also important to consider, and it would theoretically be possible that the model would be more responsive to soil moisture decreases than increases. A study by *Suarez et al.* [2014] found that precipitation was more sensitive to drying than wetting using model simulations with 12 km horizontal grid intervals and parameterized convection. However, unlike in *Suarez et al.* [2014], where the initial soil moisture was generally wet, the original NARR soil moisture data set was close to the soil wilting point in many places, especially over Kansas and Oklahoma, making soil drying experiments infeasible.

Soil moisture adjustments had a large impact on the near surface temperature and humidity, as evidenced by the relationships to the sensible and latent heat fluxes. The impact of increasing the soil moisture by $0.10\ m^3/m^3$ was the same as or greater than that resulting from a change to forested vegetation with no change in soil moisture. Figure 11 shows this for all five cases with the control vegetation adjusted soil moisture panels closer to those for the forested simulations than those from the control vegetation with no soil moisture adjustment. The 2 m mean temperature maximum was delayed in the 19 May 2010 case (Figure 5) and actually agreed better with the timing of the observed mean maximum 2 m temperature. However, because this was not seen in the other cases, it is impossible to gauge the significance of this. In terms of observations, there was no significant improvement as increasing soil moisture cooled the surface in all the cases as expected. Therefore, if the model happened to be too warm, there would be improvements, but in places where the model was close to the observations or too cool, there would be an increase in the overall error. As seen in the

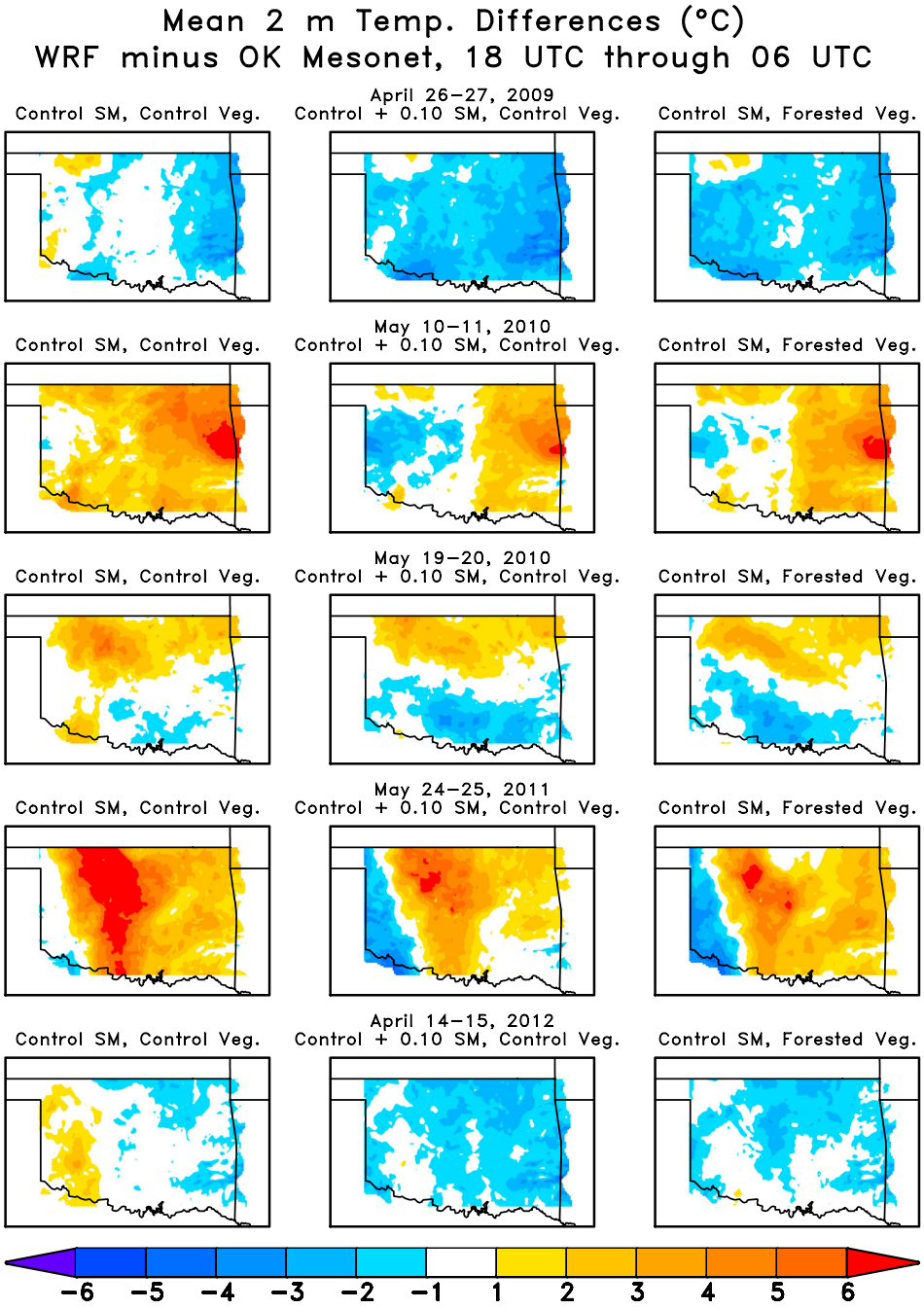

Figure 11. Mean 2 m temperature differences for the five different cases from 18 UTC through 06 UTC the next day. The left column denotes the control vegetation and NARR soil moisture (Control SM), the middle column represents the control vegetation and NARR soil moisture adjusted upward by 0.10 m^3/m^3, and the right column shows the forested vegetation with no soil moisture adjustment.

maps in Figure 11, there was no clear pattern. Figure 12 is the same as Figure 11 except for the 2 m dewpoint. Once again the same pattern was seen with soil moisture increasing the dewpoint, bringing the mean closer in line to a forested land surface than the control vegetation surface. There was no discernible pattern with regards to how increasing the soil moisture affects temperature and dewpoint for each vegetation type. Although these are model output comparisons and not necessarily true depictions of what would happen in the real world, the fact that model predicted temperature and

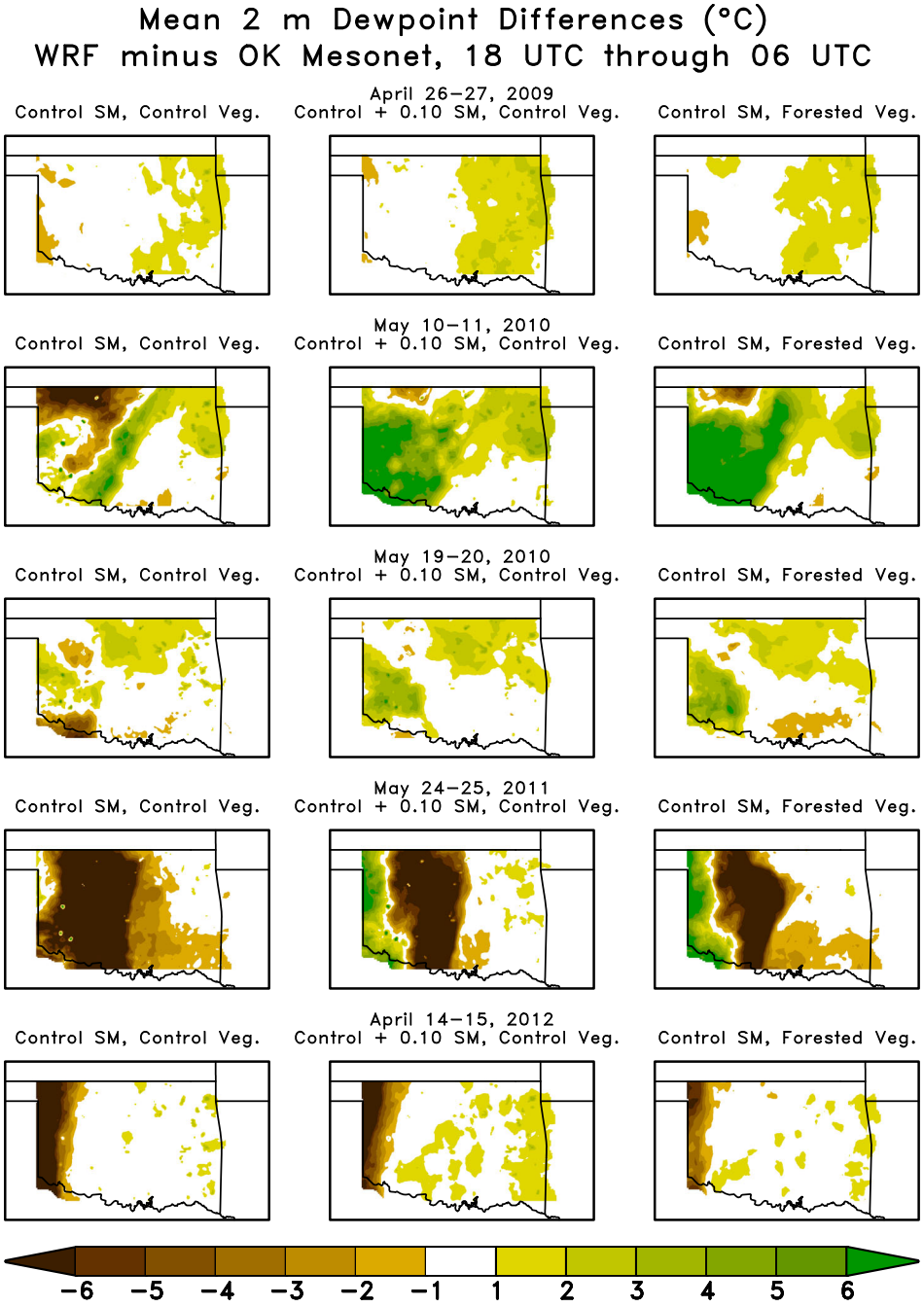

Figure 12. Same as Figure 11 except for the 2 m dewpoint.

dewpoint sensitivity to a realistic increase in soil moisture, being the same as for an unrealistic reforestation of the Great Plains is significant and illustrates the importance of soil moisture initialization.

These near surface alterations in temperature and dewpoint created changes in two variables known to impact precipitation development, namely, convective available potential energy (CAPE) and 2 m moist enthalpy. CAPE is based on the vertical profiles of temperature and dewpoint. The changes in temperature and humidity from the land surface changes occurred just near the surface and did not extend far up into the atmosphere. However, because CAPE is based on the trajectory of a lifted air parcel originating at the surface, it is intuitive that changing the temperature and humidity of the surface parcel will alter its ascent through

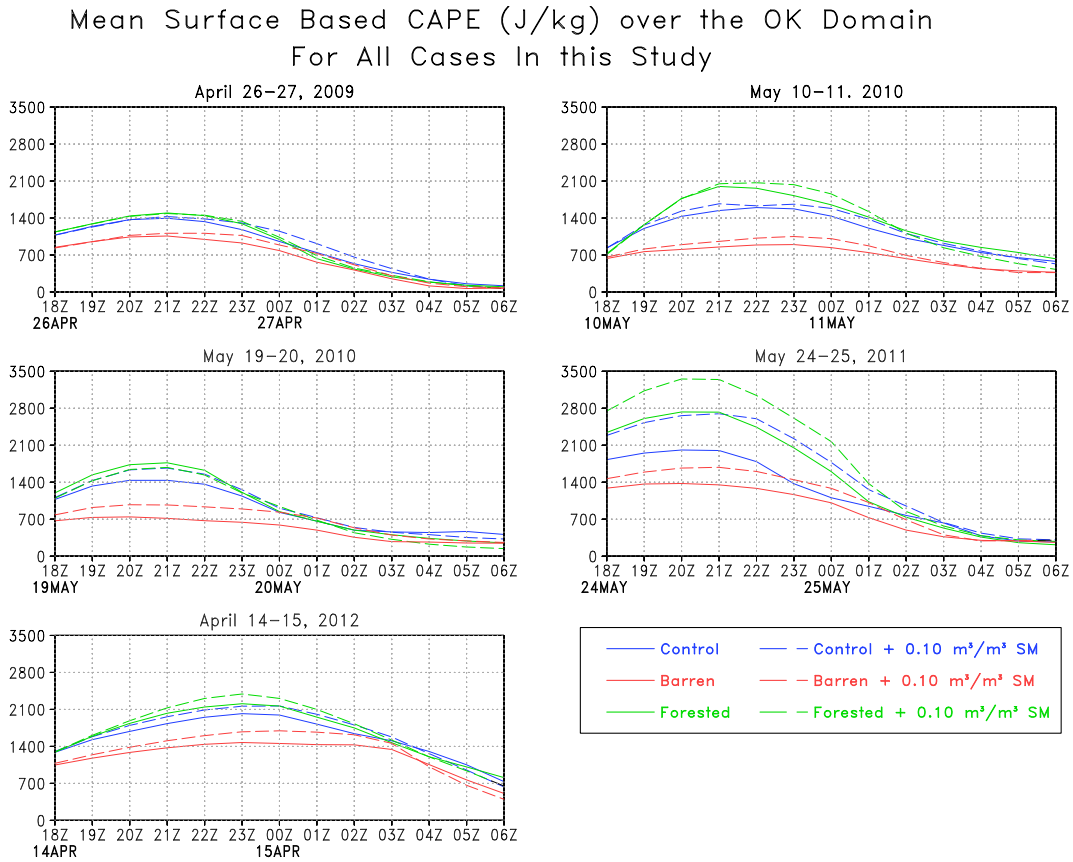

Figure 13. Time series of the mean surface based CAPE (J/kg) for all the cases in this study over the Oklahoma domain. Clockwise from top left: 26 and 27 April 2009 case, 10 and 11 May 2010 case, 24 and 25 May 2011 case, 14 and 15 April 2012 case, and 19 and 20 May 2010 case.

the atmosphere, which will induce changes in CAPE. Moist enthalpy (H) is the summation of the energy associated with the temperature and specific humidity. As defined by *Davey et al*. [2006] and *Fall et al*. [2010], the equation for H is written below.

$$H = c_p T + L_v q$$

In the above equation, T and q denote the 2 m temperature (K) and specific humidity (kilogram water vapor per kilogram air), respectively. The specific heat of air at a constant pressure, c_p, is equal to 1004 J/(Kg K), and L_v is the latent heat of vaporization (J/kg), which varies slightly with temperature. This study assumed a linear relationship based on that used by *Fall et al*. [2010].

$$L_v = [2.5 - 0.0022(T - 273.15)] * 10^6$$

Frye and Mote [2010] explained that CAPE is more sensitive to changes in moisture than temperature, and *Pielke* [2001] demonstrated that even a small increase in dewpoint has a large impact on CAPE. Figure 13 shows the time series of mean CAPE over the Oklahoma domain for each case. Generally, in each case, the patterns are similar to the precipitation patterns for each soil moisture and vegetation configuration and show that vegetation changes impact CAPE more than soil moisture changes. There did appear to be more variability in the control case for 24 May 2011, which was analogous to the precipitation patterns for that day. The 14 April 2012 case exhibited the least variability among the different vegetation classes. However, the convection for that case did not develop in the model until after 03 UTC on the 15th. By that time, the CAPE values for the different land surfaces were equalized. For this, and the other cases, the largest variability in CAPE occurred during the day. This indicated that the land surface effects on convection were more pronounced before sunset and nearly nonexistent at night. Perhaps, if convection developed earlier for the 14 April 2012 case, there would have been more variability as seen in the other cases. Figure 14 illustrates the

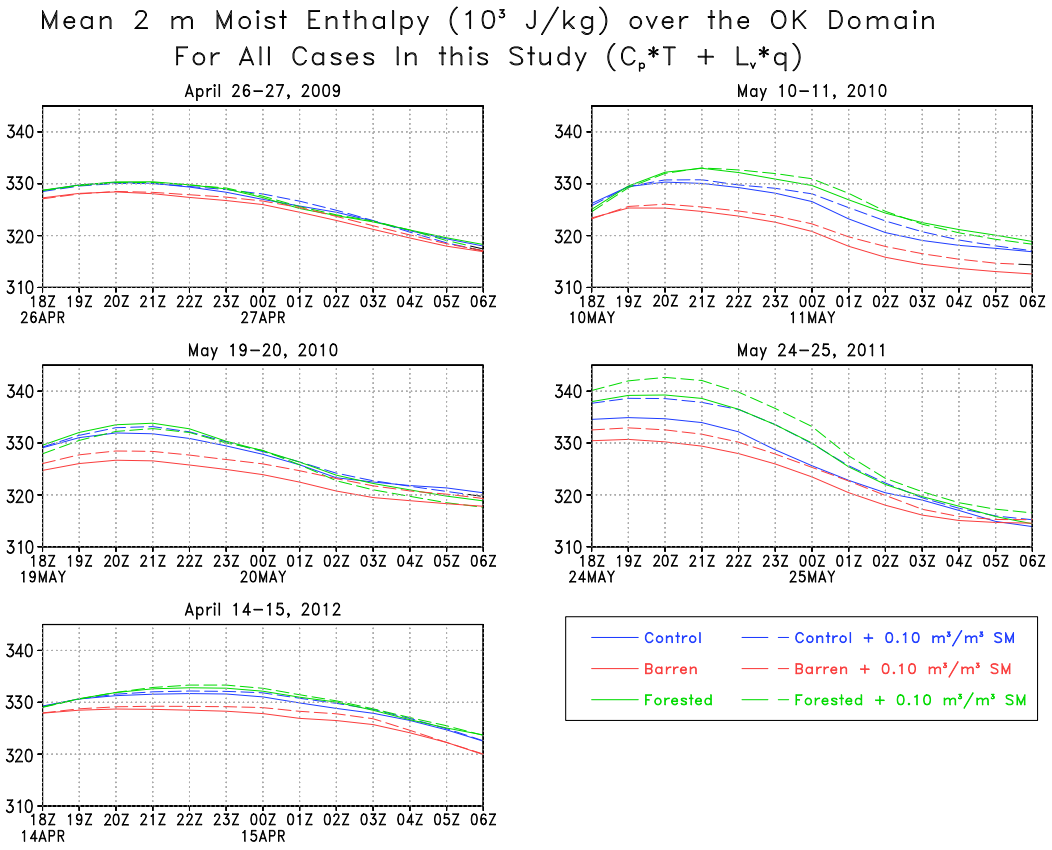

Figure 14. Same as Figure 13 except for the 2 m moist enthalpy. C_p is the specific heat at constant pressure, T is the 2 m temperature, L_v is the latent heat of vaporization, and q is the 2 m specific humidity.

moist enthalpy over the Oklahoma domain, which is similar to the CAPE time series. This showed that despite the fact that soil moisture had a similar impact individually on near surface temperature and humidity to the vegetation changes, the combined impact only led to a slight increase in moist enthalpy for each vegetation type, which also supports the limited precipitation increase.

5. Conclusions

A land surface sensitivity study using the WRF model investigated several individual convective cases with large-scale dynamical forcing and evaluated how forecasts responded to different vegetation and soil moisture initializations. Compared to the current vegetation cover, the complete removal of vegetation produced substantial drying, while conversion to forest led to modest differences in precipitation. The vegetation changes resulted in more robust changes in the mean total precipitation than the soil moisture changes. In addition, no clear pattern was observed in terms of the degree in which increased soil moisture altered precipitation for each vegetation cover as it was variable among the different cases. We discovered that NARR soil moisture is, in general, too dry, but for all of the cases, adding 0.10 m^3/m^3 to soil moisture had the same impact on 2 m temperatures and dewpoints as converting the land surface to a full forest. This upward adjustment in soil moisture did not produce any noticeable improvements in the model compared to the observations for the measures evaluated. Although, in many cases, there was a slight upward adjustment in precipitation; these changes were generally the same or less than those that result when model parameterization schemes were changed.

While it was expected that an increase in soil moisture would lead to an increase in precipitation, the individual responses of 2 m temperature and humidity were greater than the precipitation responses. It was when these two variables were combined together into convective terms such as CAPE and moist enthalpy that the decreased temperature effect and increased humidity effect that resulted from adding soil moisture

nearly negated each other only leading to slight increases of CAPE and moist enthalpy and subsequently precipitation. This shows that accurate soil moisture initialization is necessary to generate forecasts of temperature and humidity individually. Although it would appear from the figures that soil moisture is not important for precipitation forecasts for cases with strong synoptic forcing, the large impacts on temperature and dewpoint suggest that an accurate representation of soil moisture is still necessary to capture the correct balance due to the relationships between temperature, dewpoint, CAPE, and moist enthalpy. This study made an approximated adjustment to soil moisture due to the lack of in situ observations available and the desire to keep the changes uniform. However, future work will look into the responses that result from changing the soil moisture based on remotely sensed observations, which cover a large area.

Acknowledgments

This work has been supported by NASA grant NNX09AJ99G and the Brookhaven National Laboratory (BNL) Laboratory Directed Research and Development Program. Calculations were performed at the NCAR Wyoming Supercomputing Center, which is supported by the National Science Foundation. NARR data used in this study are available for download at http://rda.ucar.edu/datasets/ds608.0/. We thank Martin Schoonen (BNL) and Peter Daum (BNL) for carefully reading and editing this manuscript, Benjamin Lintner (Rutgers University) for his valuable suggestions on the analysis, and Jeffrey Basara from the University of Oklahoma for providing us with the Oklahoma Mesonet soil moisture data. We finally thank four anonymous reviewers for their feedback on earlier versions of this manuscript.

References

Ashley, W. S., M. L. Bentley, and A. Stallins (2011), Urban-induced thunderstorm modification in the Southeast United States, *Clim. Change*, *113*, 481–498, doi:10.1007/s10584-011-0324-1.

Blyth, E. M., A. J. Dolman, and J. Noilhan (1994), The effect of forest on mesoscale rainfall: An example from HAPEX-MOBILHY, *J. Appl. Meteorol.*, *33*, 445–454.

Bollasina, M., and S. Nigam (2011), Modeling of regional hydroclimate change over the Indian subcontinent: Impact of the expanding Thar desert, *J. Clim.*, *24*, 3089–3104, doi:10.1175/2010JCLI3851.1.

Case, J. L., S. V. Kumar, J. Srikishen, and G. J. Jedlovec (2011), Improving numerical weather predictions of summertime precipitation over the southeastern United States through a high-resolution initialization of the surface state, *Weather Forecasting*, *26*, 785–807, doi:10.1175/2011WAF2222455.1.

Case, J. L., J. R. Bell, F. J. LaFontaine, and C. D. Peters-Lidard (2012), Effects of real-time vegetation data on model forecasts of severe weather, paper presented at 16th Symposium on Integrated Observing and Assimilation Systems for the Atmosphere, Oceans, and Land Surface, Am. Meteorol. Soc., New Orleans, La., 15.4.

Chang, J.-T., and P. J. Wetzel (1991), Effects of spatial variations of soil moisture and vegetation on the evolution of a prestorm environment: A numerical case study, *Mon. Weather Rev.*, *119*, 1368–1390, doi:10.1175/1520-0493(1991)119<1368:EOSVOS>2.0.CO;2.

Charles, M. E., and B. A. Colle (2009), Verification of extratropical cyclones within the NCEP operational models. Part II: The short-range ensemble forecast system, *Weather Forecasting*, *24*, 1191–1214, doi:10.1175/2009WAF2222170.1.

Clark, C. A., and R. W. Arritt (1995), Numerical simulations of the effect of soil moisture and vegetation cover on the development of deep convection, *J. Appl. Meteorol.*, *34*, 2029–2045.

Comarazamy, D. E., J. E. González, J. Luvall, D. Rickman, and P. J. Mulero (2010), A land-atmospheric interaction study in the coastal tropical city of San Juan, Puerto Rico, *Earth Interact.*, *14*(16), 1–24, doi:10.1175/2010EI309.1.

Comarazamy, D. E., J. E. González, J. Luvall, D. Rickman, and R. Bornstein (2013), Climate impacts of land cover and land use changes in tropical islands under conditions of global climate change, *J. Clim.*, *26*(5), 1535–1550, doi:10.1175/JCLI-D-12-00087.1.

Coniglio, M. C., J. Correia, P. T. Marsh, and F. Kong (2013), Verification of convection-allowing WRF model forecasts of the planetary boundary layer using sounding observations, *Weather Forecasting*, *28*, 842–862, doi:10.1175/WAF-D-12-00103.1.

Crawford, T. M., D. J. Stensrud, F. Mora, J. W. Merchant, and P. Wetzel (2001), Value of incorporating satellite-derived land cover data in MM5/PLACE for simulating surface temperatures, *J. Hydrometeorol.*, *2*, 453–468.

Davey, C. A., R. A. Pielke Sr., and K. P. Gallo (2006), Differences between near-surface equivalent temperature and temperature trends for the eastern United States - Equivalent temperature as an alternative measure of heat content, *Global Planet. Change*, *54*, 19–32, doi:10.1016/j.gloplacha.2005.11.002.

DeAngelis, A., F. Dominguez, Y. Fan, A. Robock, M. D. Kustu, and D. Robinson (2010), Observational evidence of enhanced precipitation due to irrigation over the Great Plains of the United States, *J. Geophys. Res.*, *115*, D15115, doi:10.1029/2010JD013892.

Degu, A. M., F. Hossain, D. Niyogi, R. Pielke Sr., J. M. Shepherd, N. Voisin, and T. Chronis (2011), The influence of large dams on surrounding climate and precipitation patterns, *Geophys. Res. Lett.*, *38*, L04405, doi:10.1029/2010GL046482.

De Ridder, K. (1997), Land surface processes and the potential for deep convection, *J. Geophys. Res.*, *102*(D25), 30,085–30,090, doi:10.1029/97JD02624.

De Ridder, K. (1998), The impact of vegetation cover on Sahelian drought persistence, *Boundary Layer Meteorol.*, *88*, 307–321.

Doran, J. C., and S. Zhong (2000), A study of the effects of sub-grid-scale land use differences on atmospheric stability in prestorm environments, *J. Geophys. Res.*, *105*, 9381–9392, doi:10.1029/1999JD901121.

Dudhia, J. (1989), Numerical study of convection observed during the Winter Monsoon Experiment using a mesoscale two dimensional model, *J. Atmos. Sci.*, *46*, 3077–3107.

Ek, M. B., K. E. Mitchell, Y. Lin, E. Rogers, P. Grunmann, V. Koren, G. Gayno, and J. D. Tarpley (2003), Implementation of Noah land surface model advances in the National Centers for Environmental Prediction operational mesoscale Eta Model, *J. Geophys. Res.*, *108*(D22), 8851, doi:10.100.1029/2002JD003296.

Eltahir, E. A. (1998), A soil moisture–rainfall feedback mechanism: 1. Theory and observations, *Water Resour. Res.*, *34*(4), 765–776, doi:10.100.1029/97WR03499.

Entin, J. K., A. Robock, K. Y. Vinnikov, S. E. Hollinger, S. Liu, and A. Namkhai (2000), Temporal and spatial scales of observed soil moisture variations in the extratropics, *J. Geophys. Res.*, *105*, 11,865–11,877, doi:10.1029/2000JD900051.

Evans, C., R. S. Schumacher, and T. J. Galarneau (2011), Sensitivity in the overland reintensification of Tropical Cyclone Erin (2007) to near-surface soil moisture characteristics, *Mon. Weather Rev.*, *139*, 3848–3870.

Fall, S., N. Diffenbaugh, D. Niyogi, R. A. Pielke Sr., and G. Rochon (2010), Temperature and equivalent temperature over the United States (1979 - 2005), *Int. J. Climatol.*, *30*, 2045–2054, doi:10.1002/joc.2094.

Fischer, E. M., S. I. Seneviratne, P. L. Vidale, D. Lüthi, and C. Schär (2007), Soil moisture–atmosphere interactions during the 2003 European summer heat wave, *J. Clim.*, *20*, 5081–5099.

Frye, J. D., and T. L. Mote (2010), The synergistic relationship between soil moisture and the low-level jet and its role on the prestorm environment over the Southern Great Plains, *J. Appl. Meteorol. Climatol.*, *49*, 775–791, doi:10.1175/2009JAMC2146.1.

Gero, A., A. J. Pitman, G. T. Narisma, C. Jacobson, and R. A. Pielke (2006), The impact of land cover change on storms in the Sydney basin, Australia, *Global Planet. Change*, *54*, 57–78.

Grasso, L. D. (2000), A numerical simulation of dryline sensitivity to soil moisture, *Mon. Weather Rev.*, *128*, 2816–2834.
Guillod, B. P., E. L. Davin, C. Kundig, G. Smiatek, and S. I. Seneviratne (2013), Impact of soil map specifications for European climate simulations, *Clim. Dyn.*, *40*, 123–141, doi:10.1007/s00382-012-1395-z.
Hong, S.-Y., and J.-O. J. Lim (2006), The WRF single-moment 6-class microphysics scheme (WSM6), *J. Korean Meteorol. Soc.*, *42*, 129–151.
Hong, S.-Y., Y. Noh, and J. Dudhia (2006), A new vertical diffusion package with an explicit treatment of entrainment processes, *Mon. Weather Rev.*, *134*, 2318–2341, doi:10.1175/MWR3199.1.
Hong, S., V. Lakshimi, E. E. Small, F. Chen, M. Tewari, and K. W. Manning (2009), Effects of vegetation and soil moisture on the simulated land surface processes from the coupled WRF/Noah model, *J. Geophys. Res.*, *114*, D18118, doi:10.100.1029/2008JD011249.
Hossain, F., I. Jeyachandran, and R. A. Pielke Sr. (2009), Have large dams altered extreme precipitation patterns during the last Century?, *Eos Trans. AGU*, *90*, 453–455, doi:10.1029/2009EO480001.
James, K. A., D. J. Stensrud, and N. Yussouf (2009), Value of real-time vegetation fraction to forecasts of severe convection in high-resolution models, *Weather Forecasting*, *24*, 187–210.
Kain, J. S., et al. (2008), Some practical considerations regarding horizontal resolution in the first generation of operational convection-allowing NWP, *Weather Forecasting*, *23*, 931–952, doi:10.1175/WAF2007106.1.
Kim, Y., and G. Wang (2007a), Impact of initial soil moisture anomalies on subsequent precipitation over North America in the Coupled Land-Atmosphere Model CAM3-CLM3, *J. Hydrometeorol.*, *8*, 513–533, doi:10.1175/JHM611.1.
Kim, Y., and G. Wang (2007b), Impact of vegetation feedback on the response of precipitation to antecedent soil moisture anomalies over North America, *J. Hydrometeorol.*, *8*, 534–550, doi:10.1175/JHM612.1.
Koster, R. D., et al. (2006), GLACE: The global land-atmosphere coupling experiment. Part I: Overview, *J. Hydrometeorol.*, *7*, 590–610.
Kumar, P., B. K. Bhattacharya, and P. K. Pal (2013), Impact of vegetation fraction from Indian geostationary satellite on short-range weather forecast, *Agr. For. Meteorol.*, *168*, 82–92.
Kurkowski, N. P., D. J. Stensrud, and M. E. Baldwin (2003), Assessment of implementing satellite-derived land cover data in the Eta model, *Weather Forecasting*, *18*, 404–416.
Lanicci, J. M., T. N. Carlson, and T. T. Warner (1987), Sensitivity of the Great Plains severe storm environment to soil moisture distribution, *Mon. Weather Rev.*, *115*, 2660–2673.
Lin, Y., and K. E. Mitchell (2005), The NCEP stage II/IV hourly precipitation analyses: Development and applications, paper presented at 19th Conf. on Hydrology, Am. Meteorol. Soc., San Diego, Calif., 1.2.
Mahmood, R., R. Leeper, and A. Quintanar (2011), Sensitivity of planetary boundary layer atmosphere to historical and future changes of land use/land cover, vegetation fraction, and soil moisture in Western Kentucky, USA, *Global Planet. Change*, *78*, 36–53.
Matyas, C. J., and A. M. Carleton (2009), Surface radar-derived convective rainfall associations with Midwest US land surface conditions in summer seasons 1999 and 2000, *Theor. Appl. Climatol.*, *99*, 315–330, doi:10.100.1007/s00704-009-0144-7.
Mellor, G. L., and T. Yamada (1982), Development of a turbulence closure model for geophysical fluid problems, *Rev. Geophys.*, *20*(4), 851–875, doi:10.1029/RG020i004p00851.
Mesinger, F., et al. (2006), The North American regional reanalysis, *Bull. Am. Meteorol. Soc.*, *87*, 343–360, doi:10.1175/BAMS-87-3-343.
Mlawer, E. J., S. J. Taubman, P. D. Brown, M. J. Iacono, and S. A. Clough (1997), Radiative transfer for inhomogeneous atmosphere: RRTM, a validated correlated-k model for the longwave, *J. Geophys. Res.*, *102*(D14), 16,663–16,682, doi:10.1029/97JD00237.
Nie, S., Y. Luo, and Z. Jiang (2008), Trends and scales of observed soil moisture variations in China, *Adv. Atmos. Sci.*, *25*, 43–58, doi:10.1007/s00376-008-0043-3.
Pielke, R. A., Sr. (2001), Influence of the spatial distribution of vegetation and soils on the prediction of cumulus convective rainfall, *Rev. Geophys.*, *39*(2), 151–178, doi:10.1029/1999RG000072.
Pielke, R. A., and X. Zeng (1989), Influence on severe storm development of irrigated land, *Nat. Weather Dig.*, *14*(2), 16–17.
Raddatz, R. L. (1998), Anthropogenic vegetation transformation and the potential for deep convection on the Canadian prairies, *Can. J. Soil Sci.*, *78*, 657–666.
Richter, H., A. W. Western, and F. H. S. Chiew (2004), The effect of soil and vegetation parameters in the ECMWF land surface scheme, *J. Hydrometeorol.*, *5*, 1131–1146, doi:10.1175/JHM-362.1.
Sertel, E., A. Robock, and C. Ormeci (2010), Impacts of land cover data quality on regional climate simulations, *Int. J. Climatol.*, *30*, 1942–1953, doi:10.100.1002/joc.2036.
Skamarock, W. C., J. B. Klemp, J. Dudhia, D. O. Gill, D. M. Barker, M. G. Duda, X.-Y. Huang, W. Wang, and J. G. Powers (2008), A description of the Advanced Research WRF version 3, *NCAR Tech. Note, NCAR/TN-475+STR*, 125 pp., Natl. Cent. for Atmos. Res., Boulder, Colo. [Available at http://www.mmm.ucar.edu/wrf/users/docs/arw_v3.pdf.]
Stensrud, D. J., J.-W. Bao, and T. T. Warner (2000), Using initial condition and model physics perturbations in short-range ensemble simulations of mesoscale convective systems, *Mon. Weather Rev.*, *128*, 2077–2107, doi:10.1175/1520-0493(2000)128<2077:UICAMP>2.0.CO;2.
Suarez, A., R. Mahmood, A. I. Quintanar, A. Beltran-Przekurat, and R. A. Pielke Sr. (2014), A comparison of the MM5 and the RAMS simulations for land-atmosphere interactions under varying soil moisture, *Tellus A*, *66*, 1–17, doi:10.3402/tellusa.v66.21486.
Sukoriansky, S., B. Galperin, and I. Staroselsky (2005), A quasinormal scale elimination model of turbulent flows with stable stratification, *Phys. Fluids*, *17*, 085,107.
Tao, W.-K., and J. Simpson (1993), Goddard Cumulus Ensemble Model. Part I: Model description, *Terr. Atmos. Oceanic Sci.*, *4*, 35–72.
Taylor, C. M., and R. J. Ellis (2006), Satellite detection of soil moisture impacts on convection at the mesoscale, *Geophys. Res. Lett.*, *33*, L03404, doi:10.1029/2005GL025252.
Taylor, C. M., A. Gounou, F. Guichard, P. P. Harris, R. J. Ellis, F. Couvreux, and M. De Kauwe (2011), Frequency of Sahelian storm initiation enhanced over mesoscale soil-moisture patterns, *Nat. Geosci.*, *4*, 430–433, doi:10.1038/ngeo1173.
Taylor, C. M., R. A. M. de Jeu, F. Guichard, P. P. Harris, and W. A. Dorigo (2012), Afternoon rain more likely over drier soils, *Nature*, *489*, 423–426, doi:10.1038/nature11377.
Taylor, C. M., C. E. Birch, D. J. Parker, N. Dixon, F. Guichard, G. Nikulin, and G. M. S. Lister (2013), Modeling soil moisture-precipitation feedback in the Sahel: Importance of spatial scale versus convective parameterization, *Geophys. Res. Lett.*, *40*, 6213–6218, doi:10.1002/2013GL058511.
Trail, M., et al. (2013), Potential impact of land use change on future regional climate in the Southeastern U.S.: Reforestation and crop land conversion, *J. Geophys. Res. Atmos.*, *118*, 11,577–11,588, doi:10.100.1002/2013JD020356.
Vinnikov, K. Y., A. Robock, N. A. Speranskaya, and C. A. Schlosser (1996), Scales of temporal and spatial variability of midlatitude soil moisture, *J. Geophys. Res.*, *101*, 7163–7174, doi:10.1029/95JD02753.
Wang, W., B. T. Anderson, N. Phillips, R. K. Kaufmann, C. Potter, and R. B. Myneni (2006), Feedbacks of vegetation on summertime climate variability over the North American grasslands. Part I: Statistical analysis, *Earth Interact.*, *10*(17), 1–27, doi:10.1175/EI196.1.

Weaver, C. P., and R. Avissar (2001), Atmospheric disturbances caused by human modification of the landscape, *Bull. Am. Meteorol. Soc.*, *82*, 269–281.

Woldemichael, A., F. Hossain, R. A. Pielke Sr., and A. Beltran-Przekurat (2012), Understanding the impact of dam-triggered land use/land cover change on the modification of extreme precipitation, *Water Resour. Res.*, *48*, W09547, doi:10.1029/2011WR011684.

Woldemichael, A. T., F. Hossain, and R. A. Pielke Sr. (2014), Impacts of post-dam land-use/land-cover changes on modification of extreme precipitation in contrasting hydro-climate and terrain features, *J. Hydrometeorol.*, *15*, 777–800, doi:10.1175/JHM-D-13-085.1.

Yu, E., H. Wang, J. Sun, and Y. Gao (2012), Climatic response to changes in vegetation in the Northwest Hetao Plain as simulated by the WRF model, *Int. J. Climatol.*, *33*, 1470–1481, doi:10.100.1002/joc.3527.